Nuclear Clustering and Non-Equilibrium Dynamics in Small-System Collisions

Xinli Zhao (赵新丽)

University of Shanghai for Science and Technology (上海理工大学)

arXiv: 2404.09780v2

In Collaboration with:

Ziwei Lin, You Zhou, Chao Zhang (张潮) , Guoliang Ma (马国亮)

24-28, October

Cluster Structures

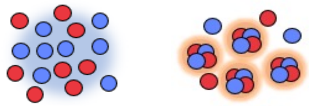

Nucleosynthesis in astrophysics

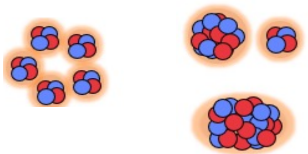

Nuclear excitation

During the nuclear excitation, phase transitions occur then form nuclear clusters.

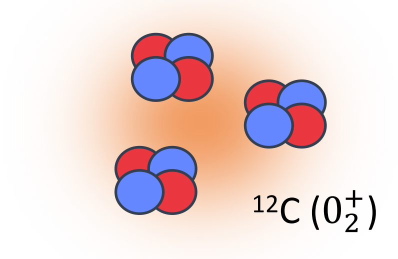

3α Bose-Einstein condensate

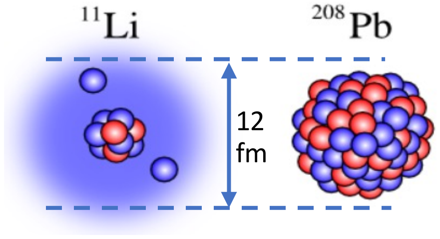

Halo type for ^{11}Li

^{20}Ne

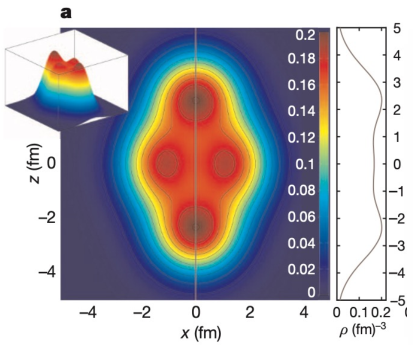

J.P. Ebran et al. Nature487, 341(2012)

^{16}O

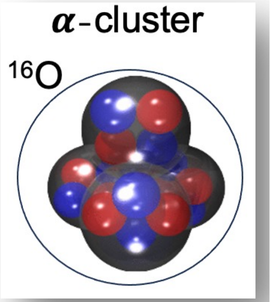

Cluster Structures

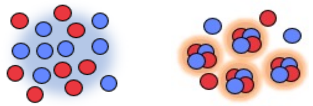

Nucleosynthesis in astrophysics

During the nuclear excitation, phase transitions occur then form nuclear clusters.

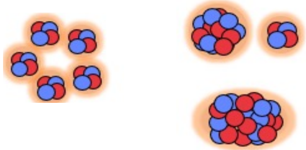

Nuclear excitation

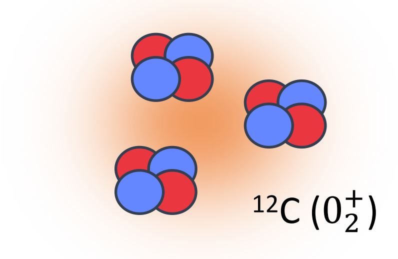

3α Bose-Einstein condensate

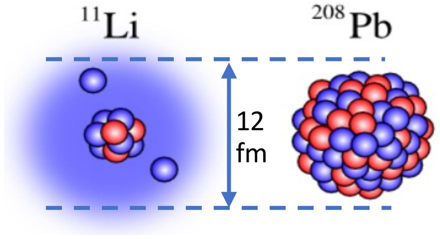

Halo type for ^{11}Li

^{20}Ne

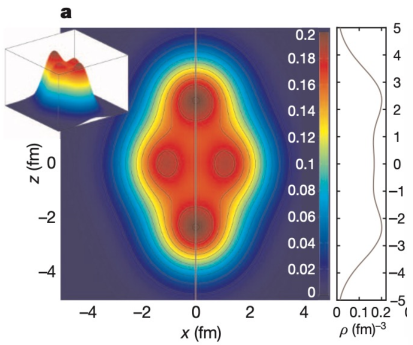

^{16}O

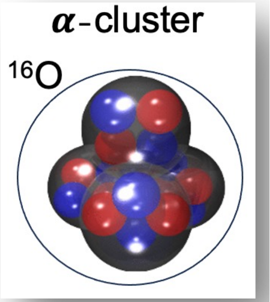

J.P. Ebran et al. Nature487, 341(2012)

STAR, Nature 635, 67 (2024)

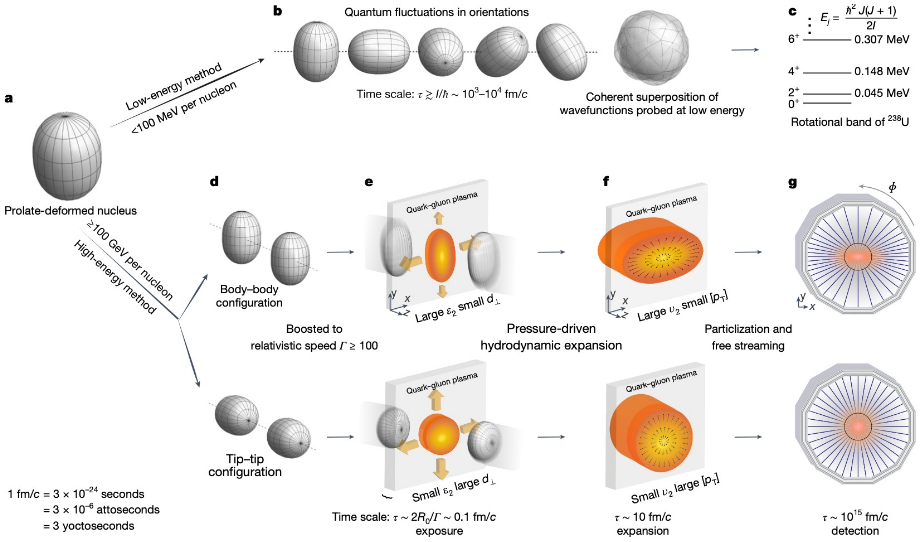

Cluster Structures

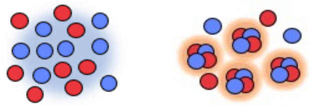

Nucleosynthesis in astrophysics

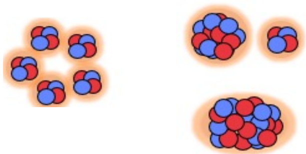

Nuclear excitation

During the nuclear excitation, phase transitions occur then form nuclear clusters.

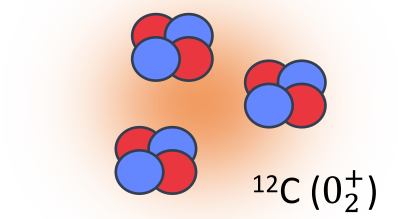

3α Bose-Einstein condensate

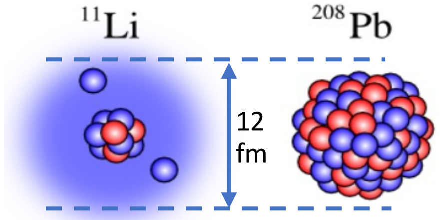

Halo type for ^{11}Li

^{20}Ne

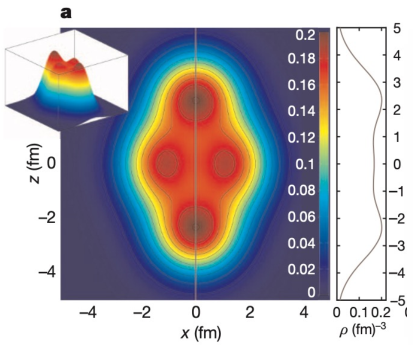

^{16}O

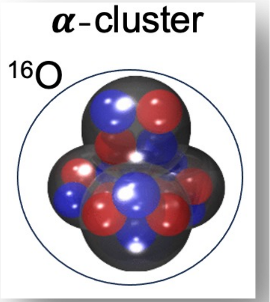

J.P. Ebran et al. Nature487, 341(2012)

STAR, Nature 635, 67 (2024)

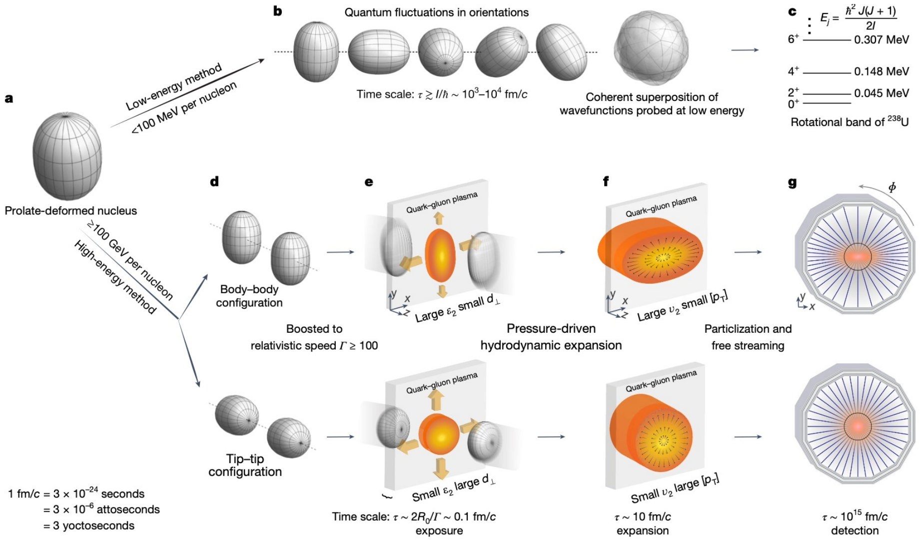

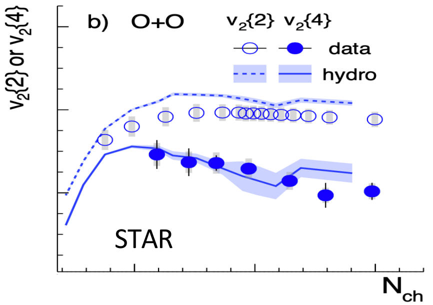

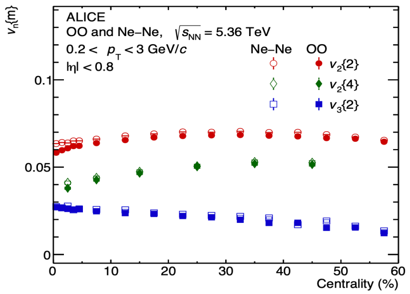

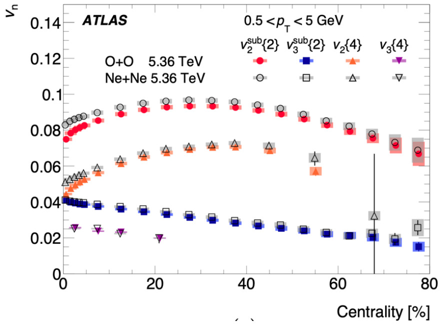

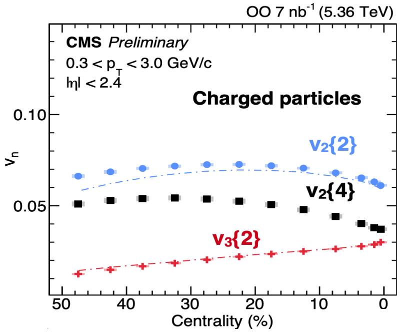

STAR, arXiv:2510.19645
ALICE, arXiv:2509.06428
ATLAS, arXiv:2509.05171
CMS, arXiv:2510.02580

Cluster Structures

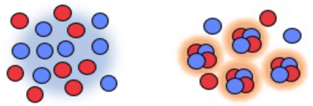

Nucleosynthesis in astrophysics

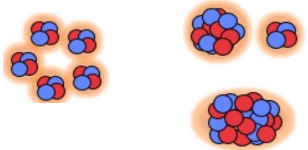

Nuclear excitation

During the nuclear excitation, phase transitions occur then form nuclear clusters.

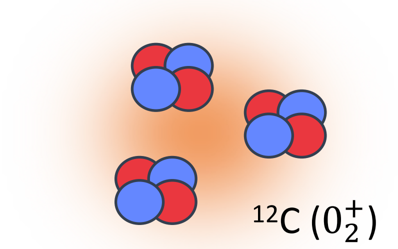

3α Bose-Einstein condensate

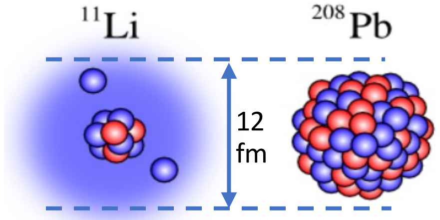

Halo type for ^{11}Li

^{20}Ne

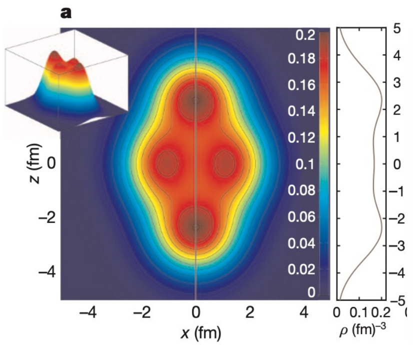

J.P. Ebran et al. Nature487, 341(2012)

^{16}O

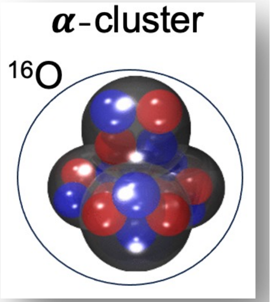

STAR, Nature 635, 67 (2024)

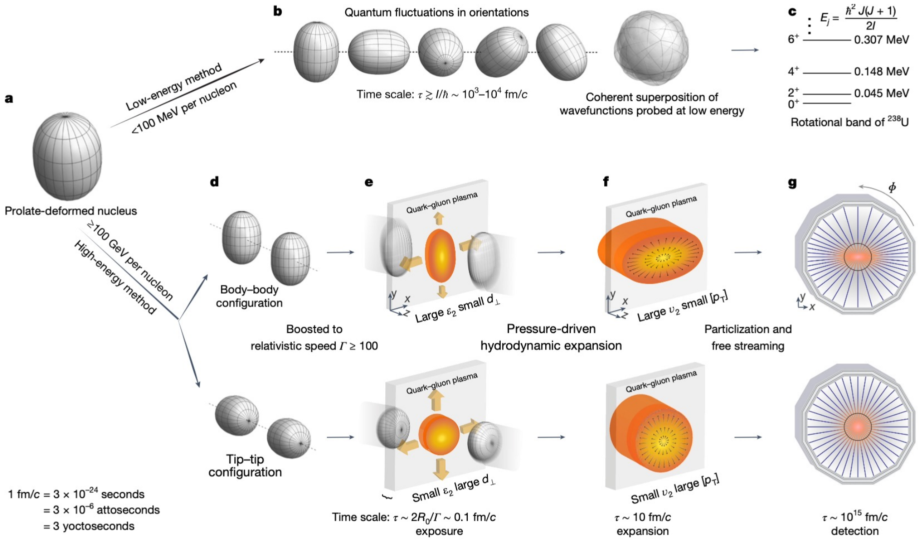

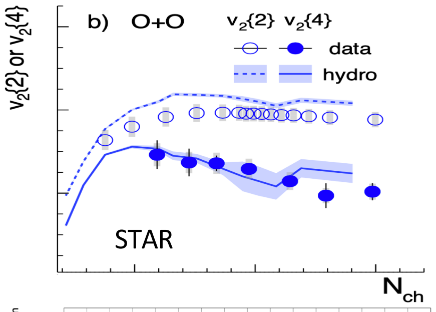

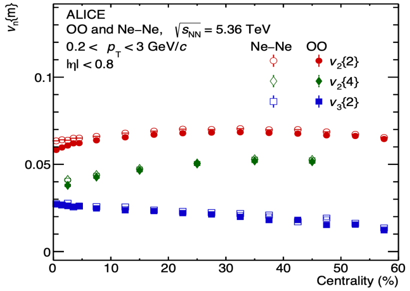

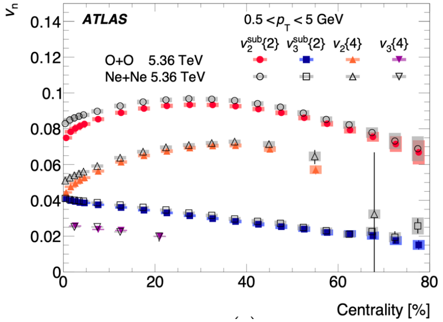

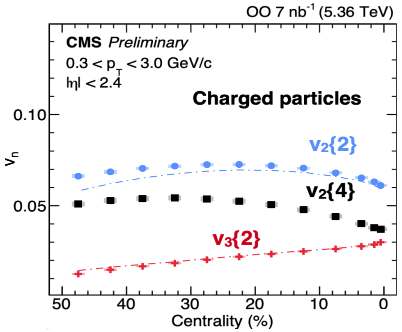

STAR, arXiv:2510.19645
ALICE, arXiv:2509.06428
ATLAS, arXiv:2509.05171
CMS, arXiv:2510.02580

- Nuclear structure effects help better constrain the collective flow of the QGP and strengthen the interdisciplinary link between nuclear structure and high-energy QCD.

Collective Flow & Nuclear Structure

$$\rho(r,\theta,\phi) = \frac{\rho_0}{1+e^{(r-R(\theta,\phi))/a_0}}$$

$$R(\theta,\phi) = R_0(1+\beta_2[\cos\gamma Y_{2,0}(\theta,\phi)+\sin\gamma Y_{2,2}(\theta,\phi)]+\beta_3 Y_{3,0}(\theta,\phi)+\beta_4 Y_{4,0}(\theta,\phi))$$

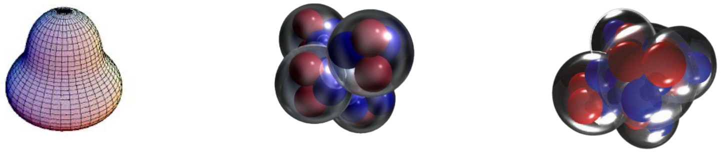

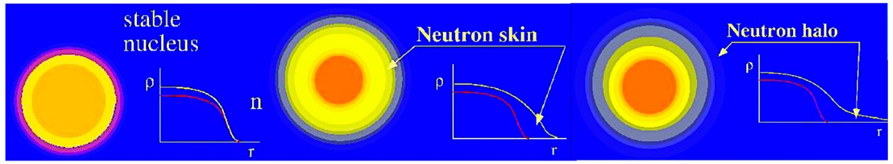

Initial Geometry

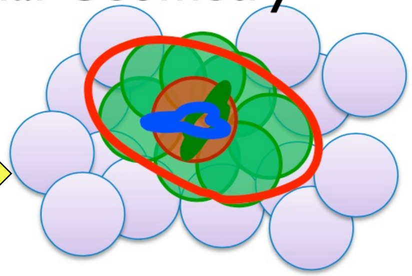

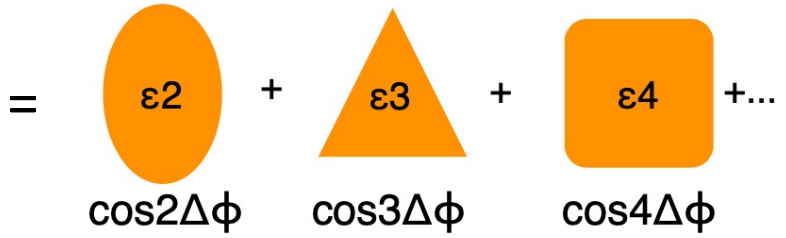

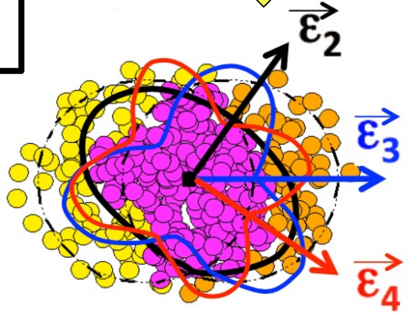

Hydro-response

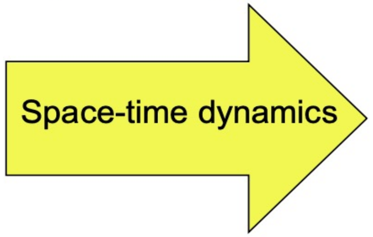

Particle distribution

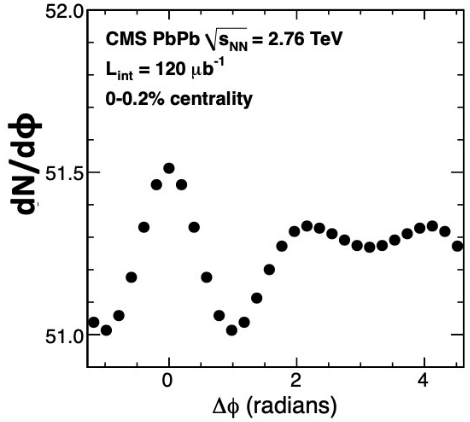

Initial size Initial shape

$R_\perp^2 \propto \langle r_\perp^2 \rangle$ $\quad \mathcal{E}_n \propto \langle r_\perp^n e^{in\phi} \rangle$

$R_0 \quad a_0 \quad \beta_n$

From J.Y. Jia's talk

Approximate linear response: $\frac{\delta[p_T]}{[p_T]} \propto -\frac{\delta R_\perp}{R_\perp}$ $\quad V_n \propto \mathcal{E}_n$

➢ Image the shape and radial profile of nuclei using the hydrodynamic response.

Motivation of Transport Model for Small Systems

$\mathbf{Pb + Pb}$

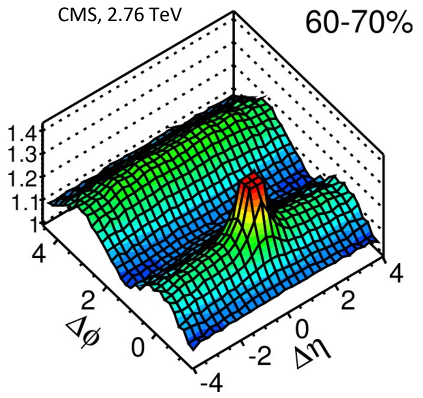

CMS, EPJC (2012) 72:2012

$\boldsymbol{p} + \mathbf{Pb}$

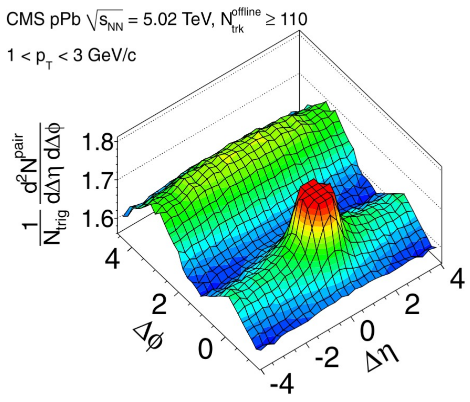

CMS, PLB 718 (2013) 795–814

$\boldsymbol{p} + \boldsymbol{p}$

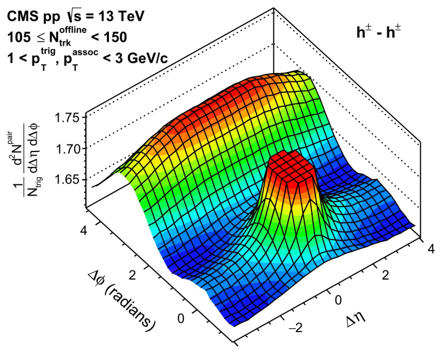

CMS, PLB 765 (2017) 193–220

- Near side ridges are indication of collectivity in small systems.

1) Are they the real collectivity signals?
2) Is the QGP formed in small systems?

Motivation of Transport Model for Small Systems

Pb + Pb

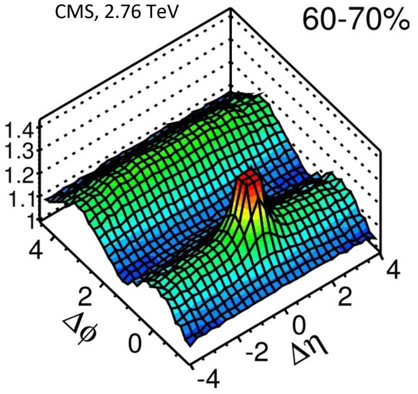

CMS, EPJC (2012) 72:2012

***p* + Pb**

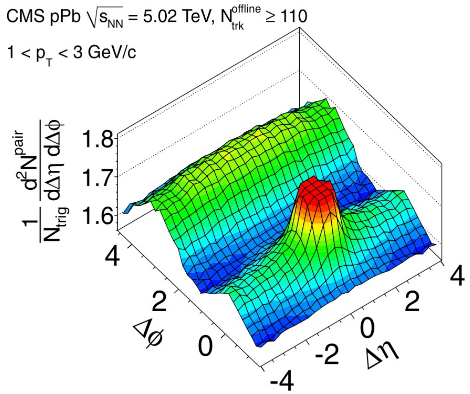

CMS, PLB 718 (2013) 795–814

p* + *p

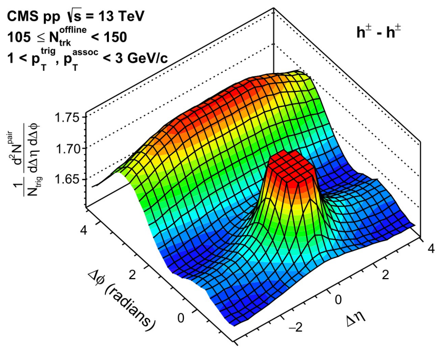

CMS, PLB 765 (2017) 193–220

- ➢ Near side ridges are indication of collectivity in small systems.

1) Are they the real collectivity signals?
2) Is the QGP formed in small systems?

Large systems → Small systems

Large systems	Small systems	
Pb+Pb	O+O	p+A
U+U	Ne+Ne	d+A
Au+Au	Ca+Ca	He+A
Xe+Xe	…	…
…		

- ➢ **For large systems**
- ✓ Transport models are similar to hydrodynamics and work very well.
- ➢ **2) For finite/small systems**
- ✓ Non-equilibrium effects are expected to be important.

- ➢ To study the properties of parton matter in small systems, transport models are crucial as they address non-equilibrium dynamics.

String Melting Version of A Multi-Phase Transport Model (AMPT)

- A transport model for non-equilibrium.
- AMPT is designed to be a self-contained kinetic description of nuclear collisions.
- Automatically includes non-equilibrium initial state & dynamics/evolution.

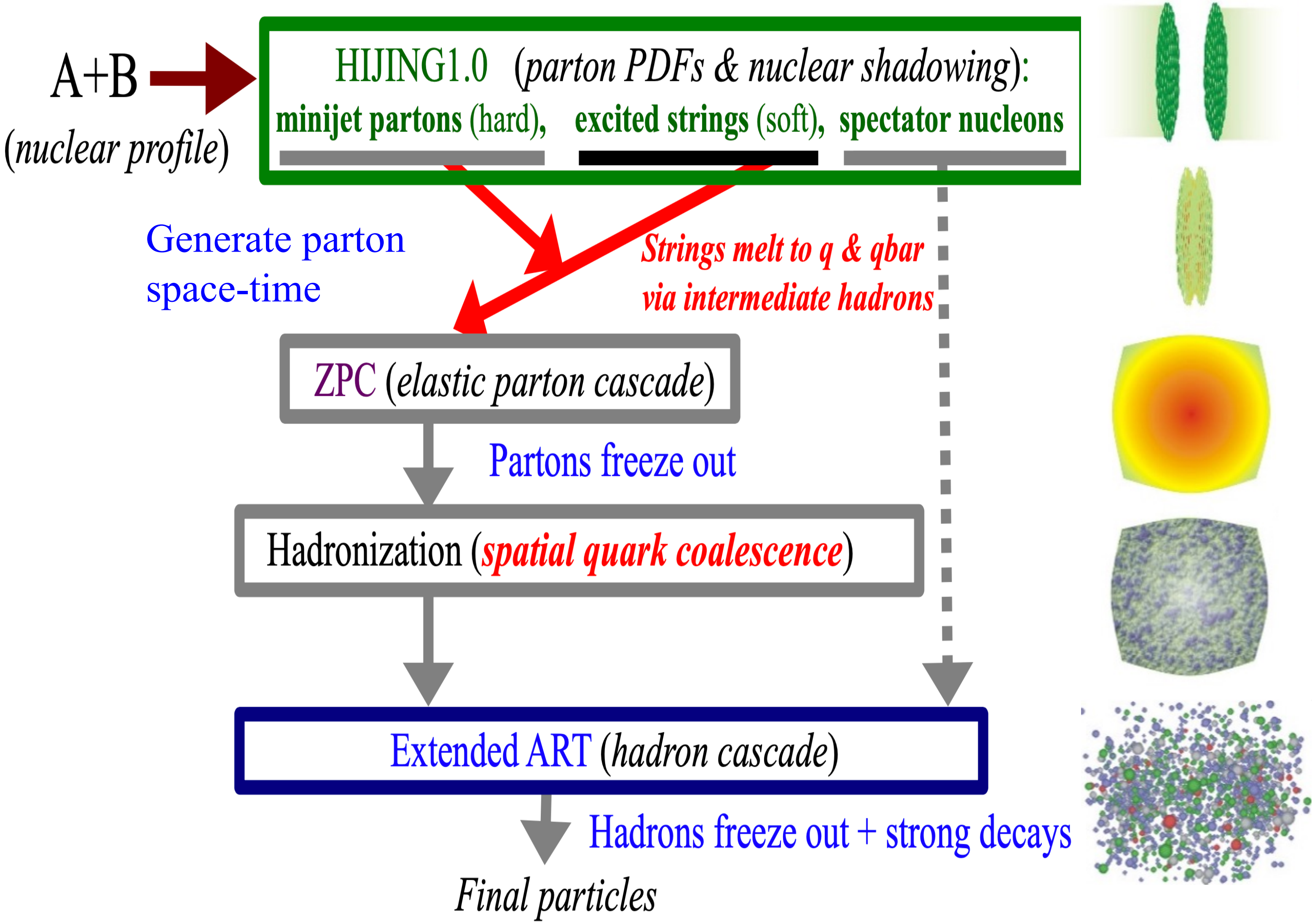

Z.W. Lin, Phys. Rev. C 72 (2005) 064901.

Nuclear Structure for ^{16}O in improved AMPT

1) New quark coalescence model
2) Improved heavy quark productions
3) Modern PDFs, nuclear shadowing and Local nuclear scaling

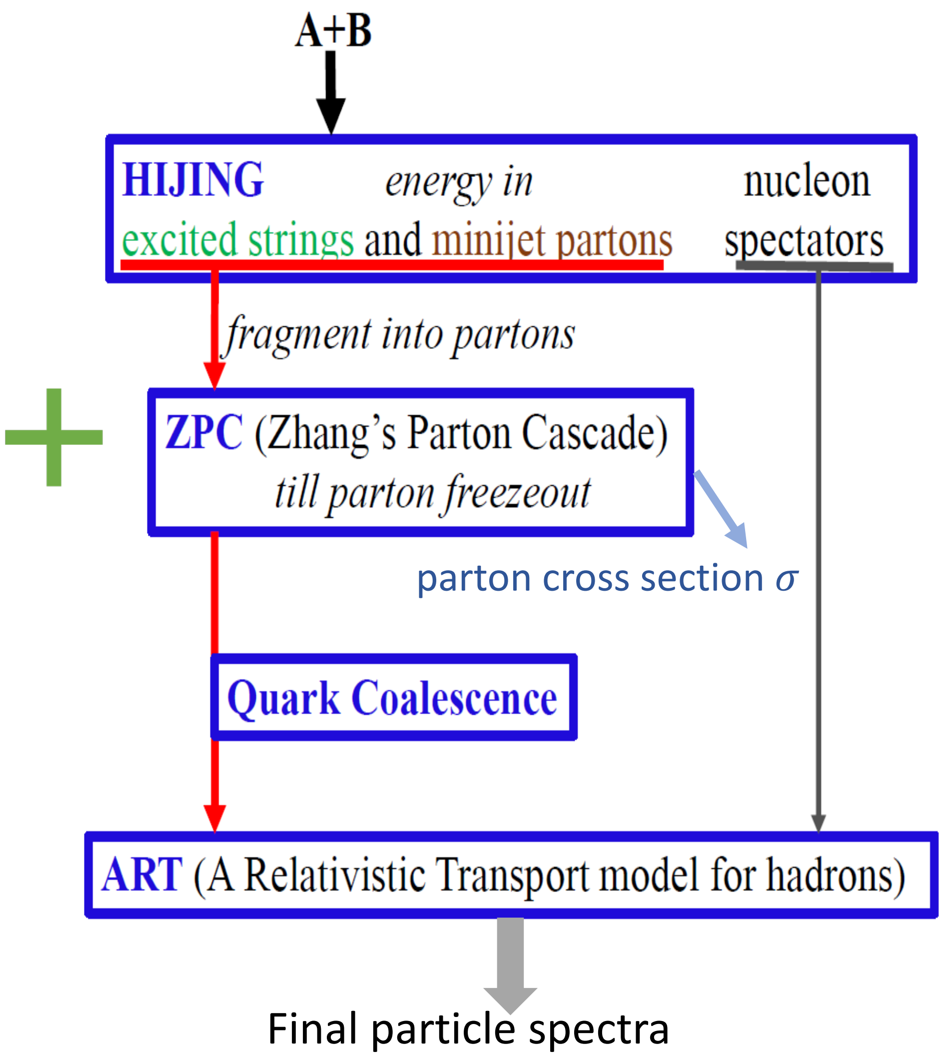

Nuclear Structure for ^{16}O in improved AMPT

1) New quark coalescence model
2) Improved heavy quark productions
3) Modern PDFs, nuclear shadowing
   and Local nuclear scaling

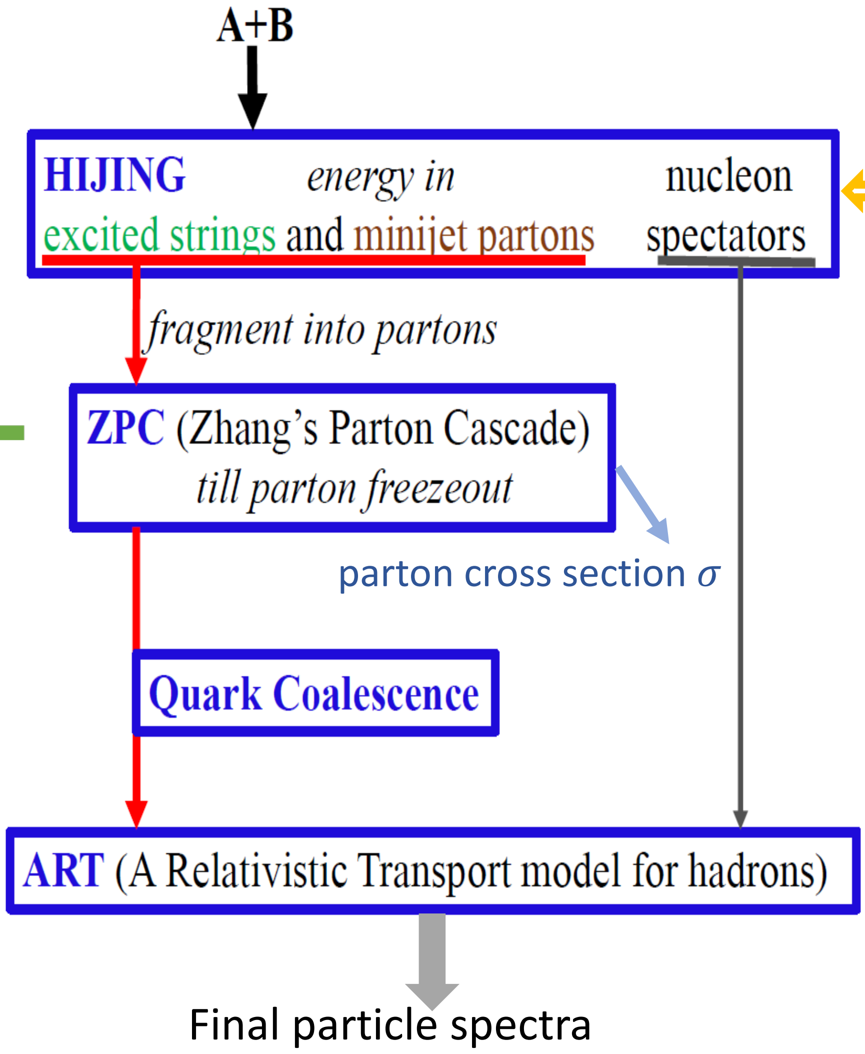

Constraint: $\langle r^2 \rangle^{1/2} = 2.6991$ fm

1. Woods-Saxon

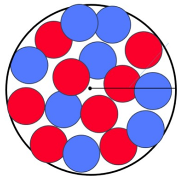

2. Tetrahedron

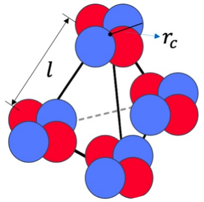

3. Square

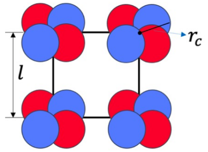

4. *ab initio* method (NLEFT)

N. Summerfield, B.-N. Lu, C. Plumberg, D. Lee, J. Noronha-Hostler, and A. Timmins, Phys. Rev. C 104, L041901 (2021), 2103.03345.

$\langle p_T \rangle$ & v_2 for $^{16}O + ^{16}O$ at 200 GeV

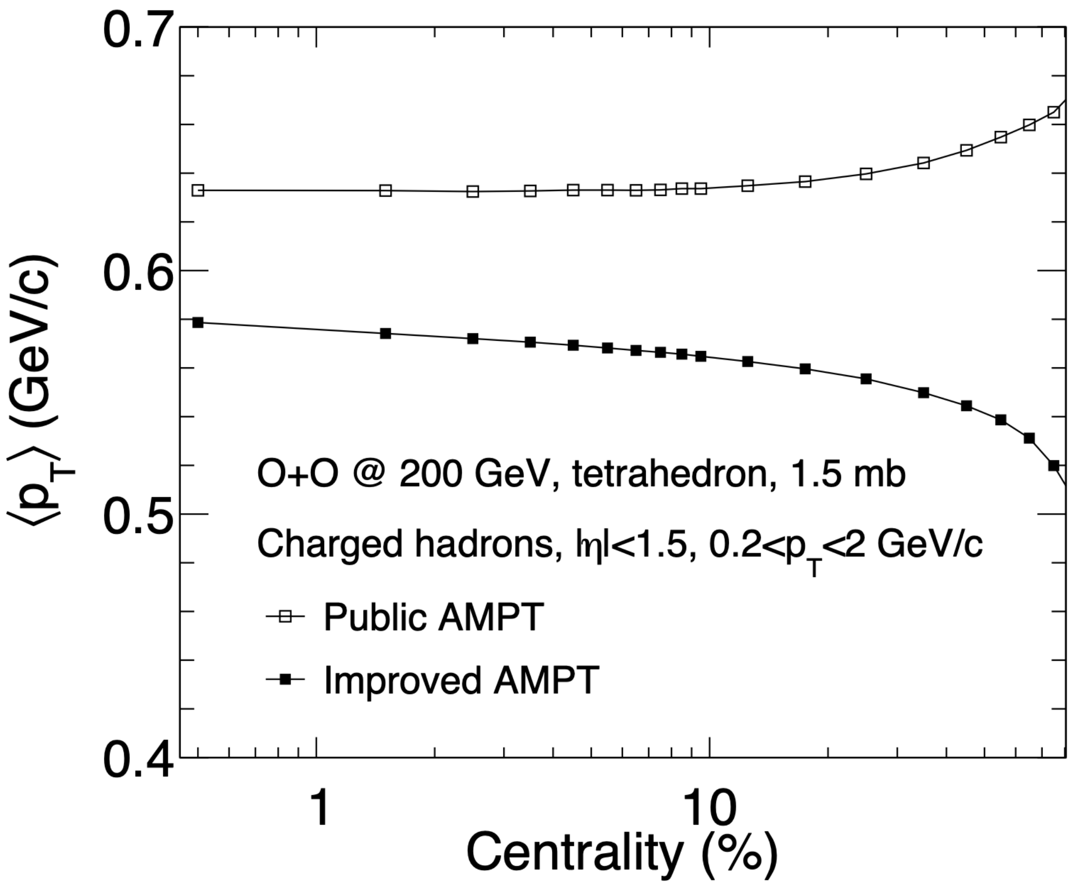

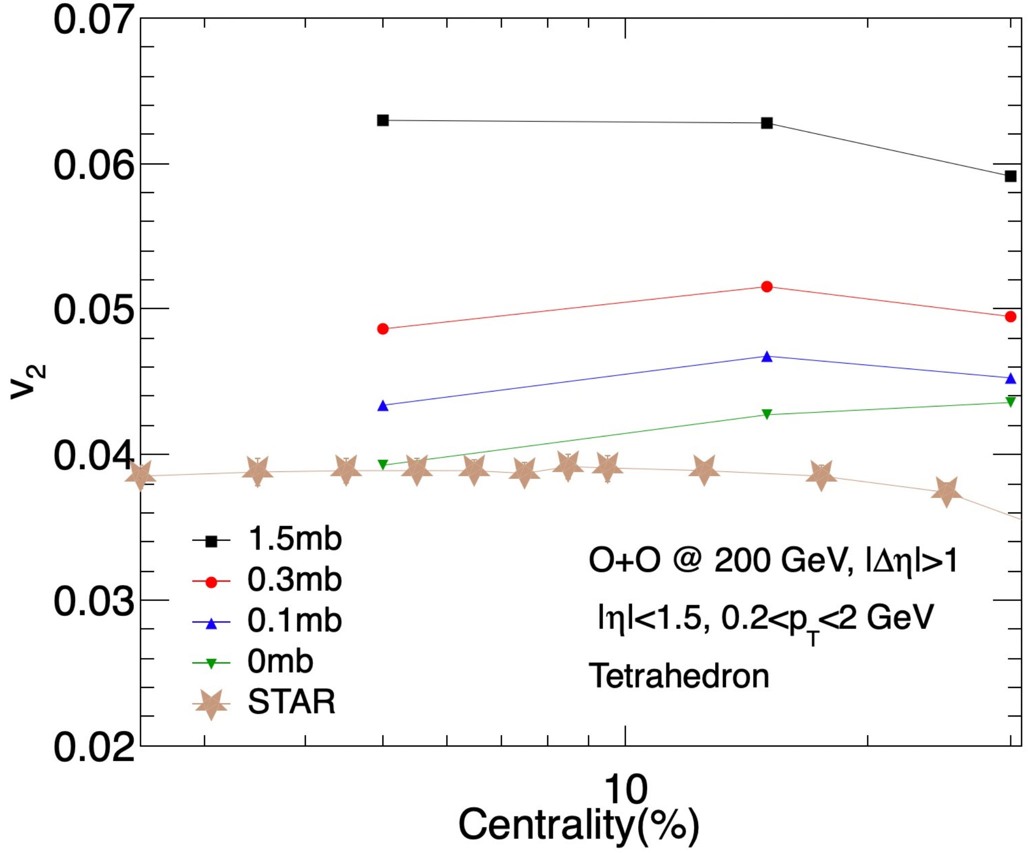

- In improved AMPT, $\langle p_T \rangle$ is reasonable but v_2 is higher than data.
- **v_2 is sensitive to the hadron effect.**

Problem of Hadronization at 200 GeV

Problem:

in AMPT-SM, hadronization starts when parton interactions stop, not at a given energy density.

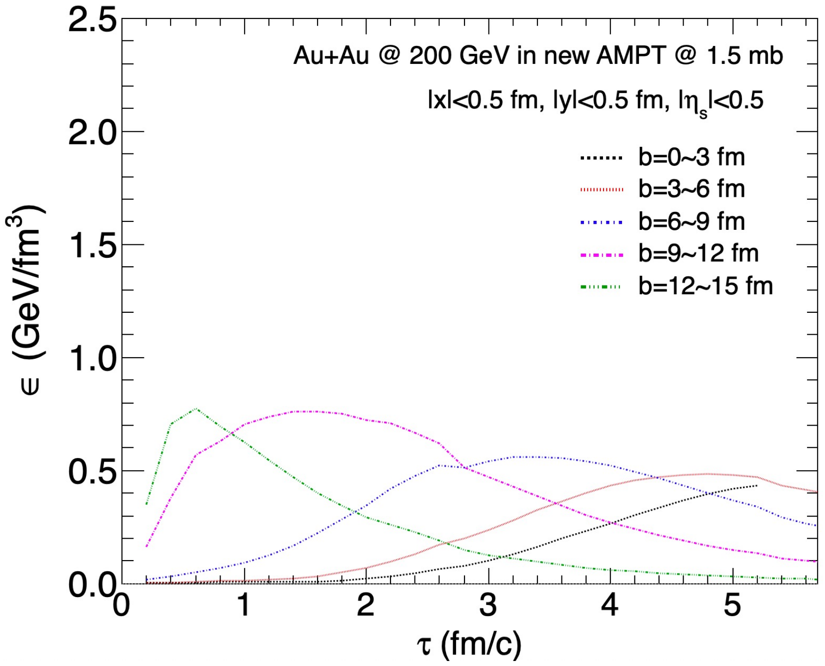

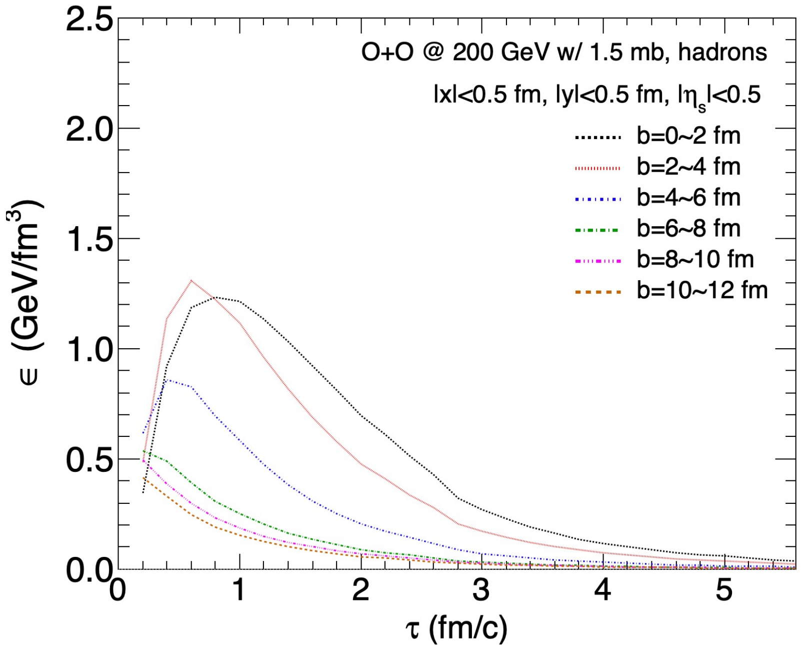

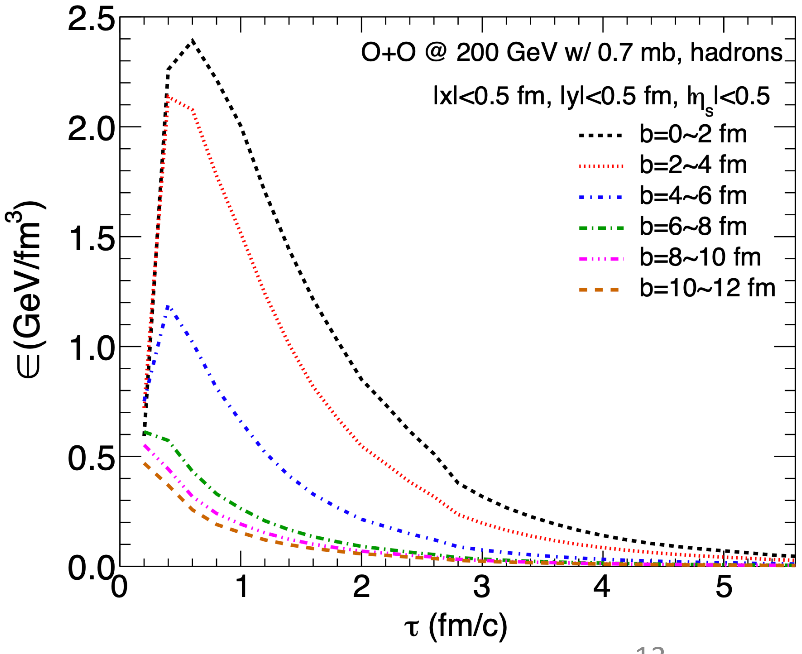

Problem of Hadronization at 200 GeV

Problem:	Qualitative estimate:
in AMPT-SM, hadronization starts when parton interactions stop, not at a given energy density.	parton interactions stop when $\sigma n L \sim 1$ $n \sim \frac{1}{\sigma L}$ is higher for a smaller system n : parton density L : system size

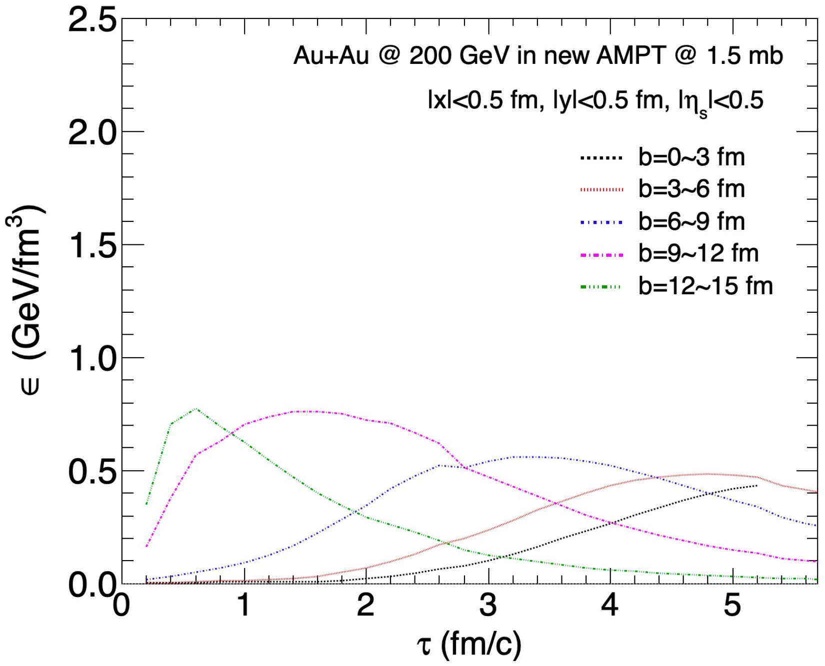

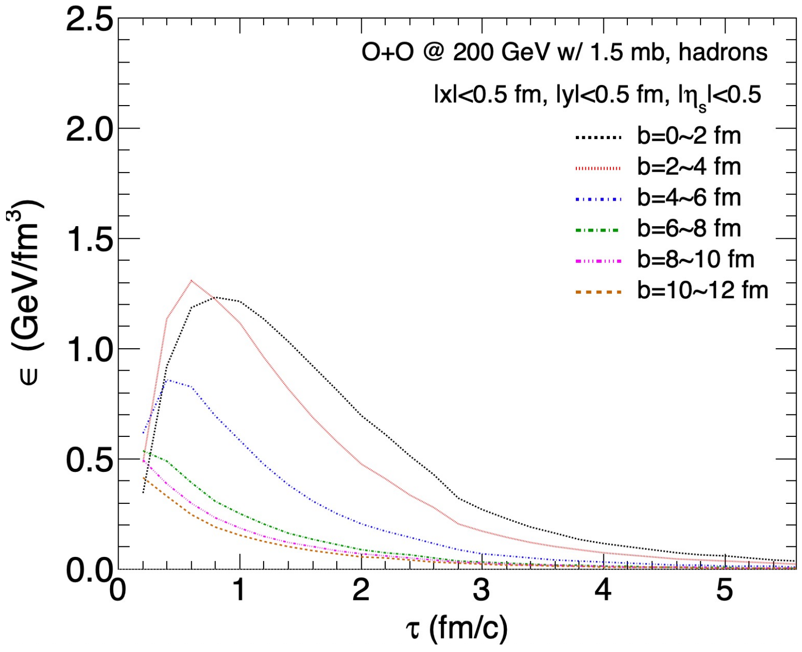

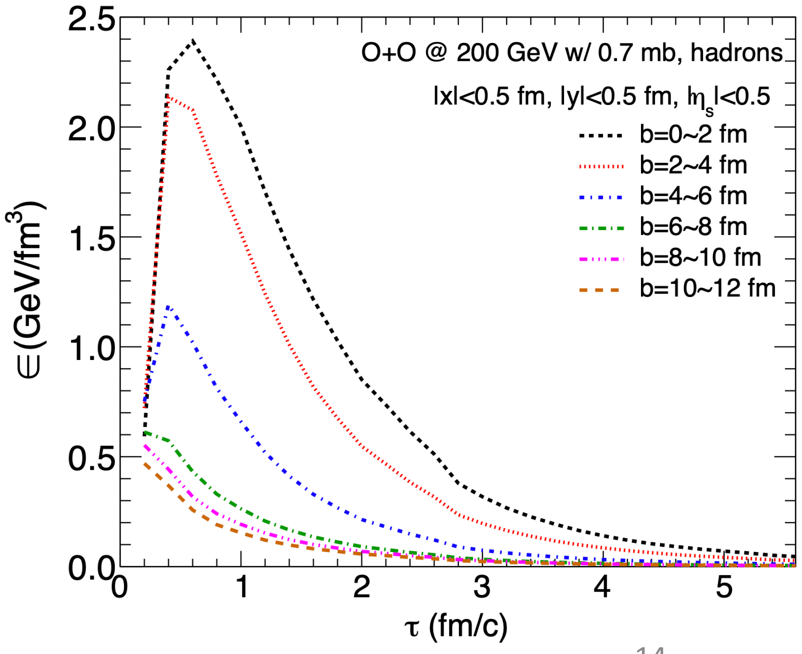

Solution of Hadronization Problem at 200 GeV

- Increasing hadron proper formation time by $\Delta\tau_{\mathrm{hadron}}$.

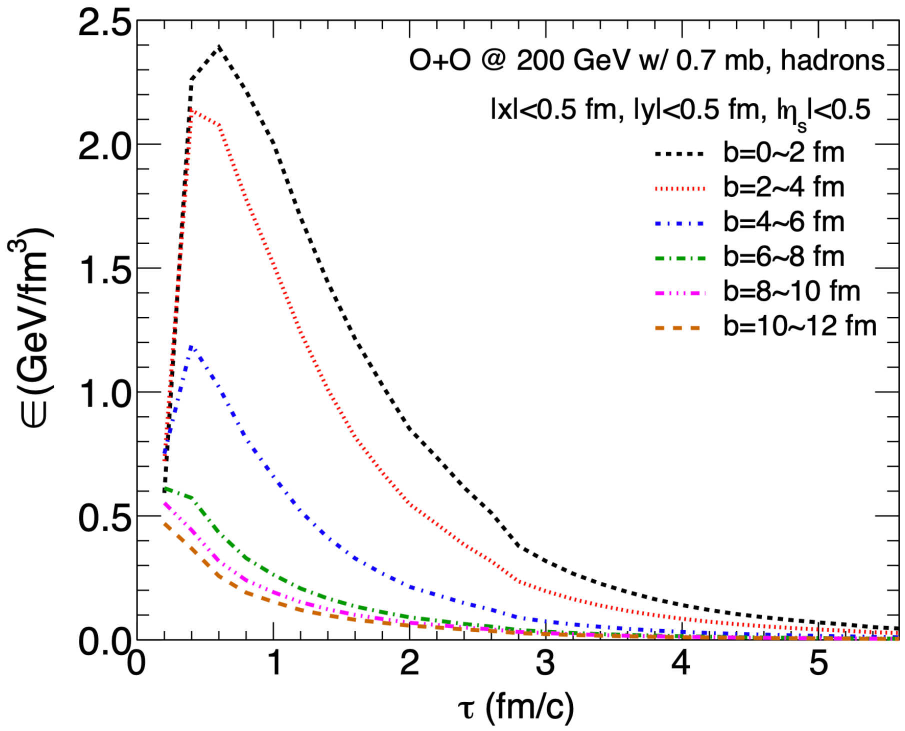

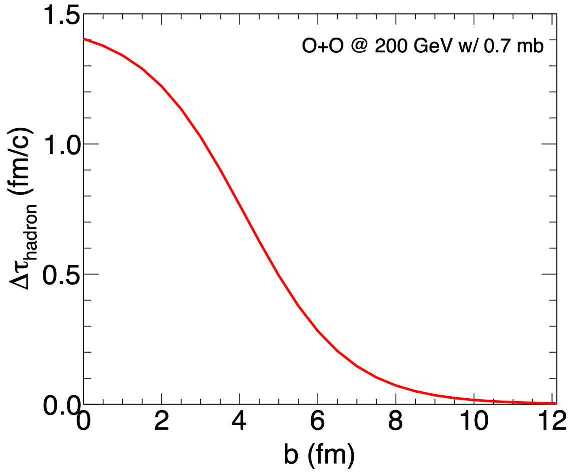

Solution of Hadronization Problem at 200 GeV

- Increasing hadron proper formation time by $\Delta\tau_{\mathrm{hadron}}$.
- The peak hadronic energy density is around a fixed $\epsilon_c \approx 0.3\ \mathrm{GeV/fm^3}$.

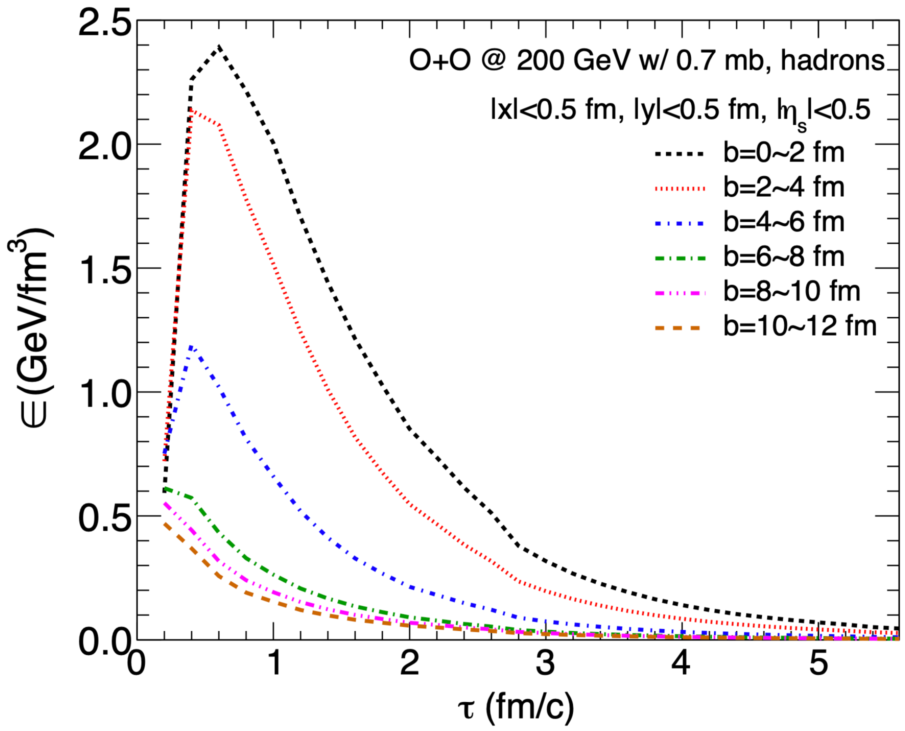

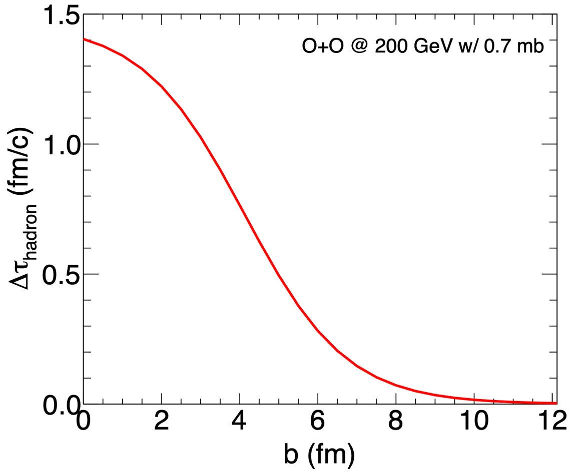

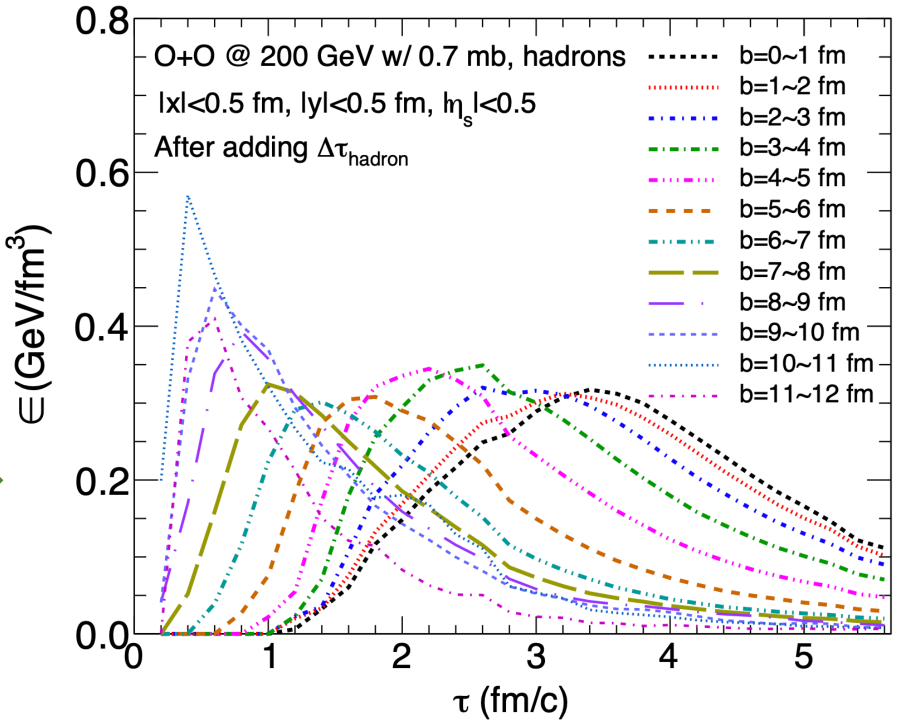

ε_n & v_n Results for ^{16}O+ ^{16}O at 200 GeV

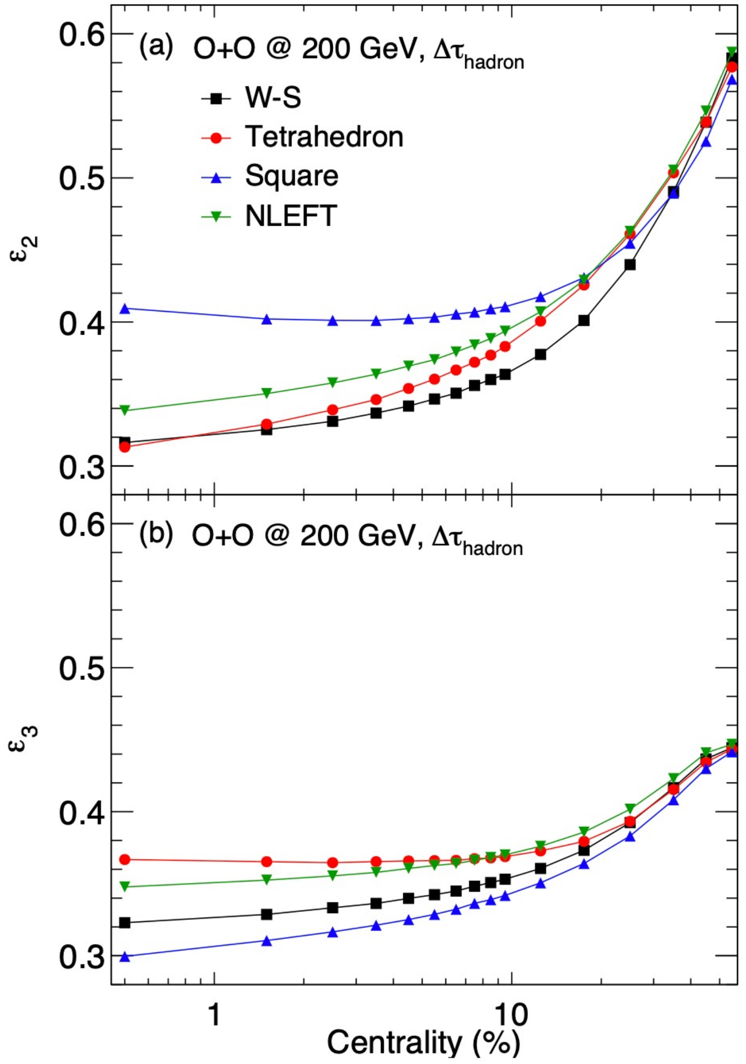

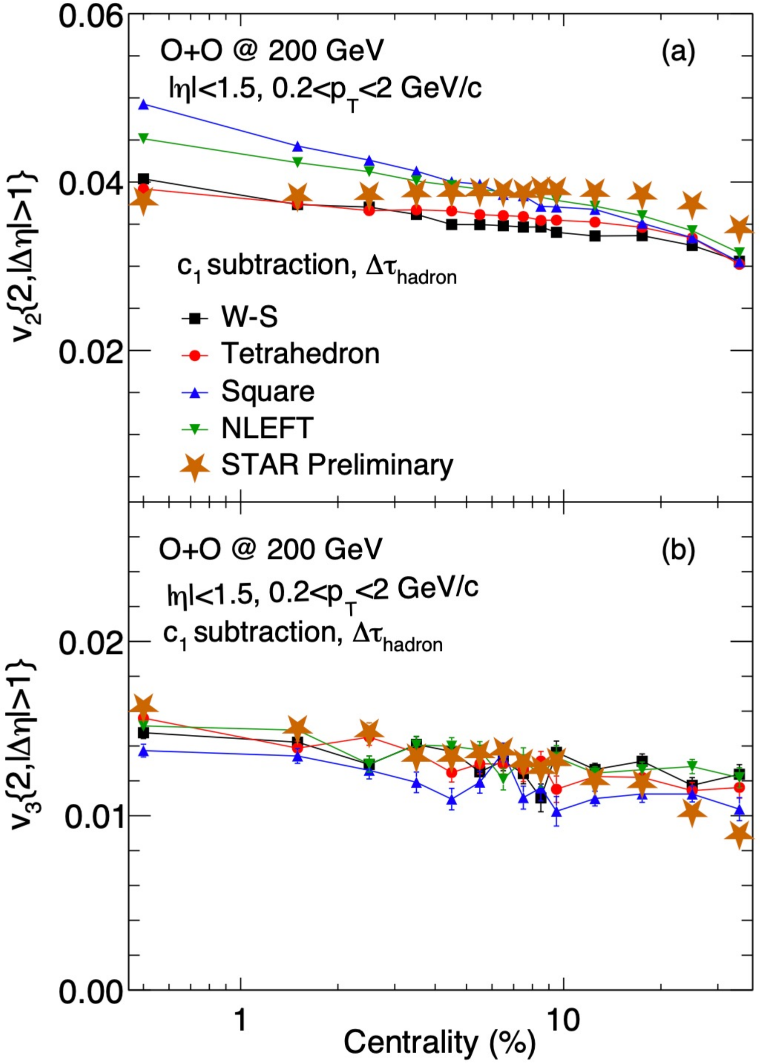

- The non-flow subtraction methods

$$\frac{dN^{\mathrm{pairs}}}{d\Delta\phi} \propto 1 + 2\sum_{n=1}^{\infty} v_n \cos(n\Delta\phi)$$

$$Y(\Delta\phi, p_{\mathrm{T}}^{\mathrm{trig}}) = c_0(1 + 2\sum_{n=1}^{n=4} c_n \cos(n\Delta\phi))$$

$$c_n^{\mathrm{sub}} = c_n - c_n^{\mathrm{non-flow}} = c_n^{\mathrm{cent}} - c_n^{\mathrm{peri}} \times f$$

- v_2 is sensitivity to nuclear structure effects at central collisions.
- v_3 is insensitivity to nuclear structure effects.

$v_n(p_T)$ Results for $^{16}O+^{16}O$ at 200 GeV

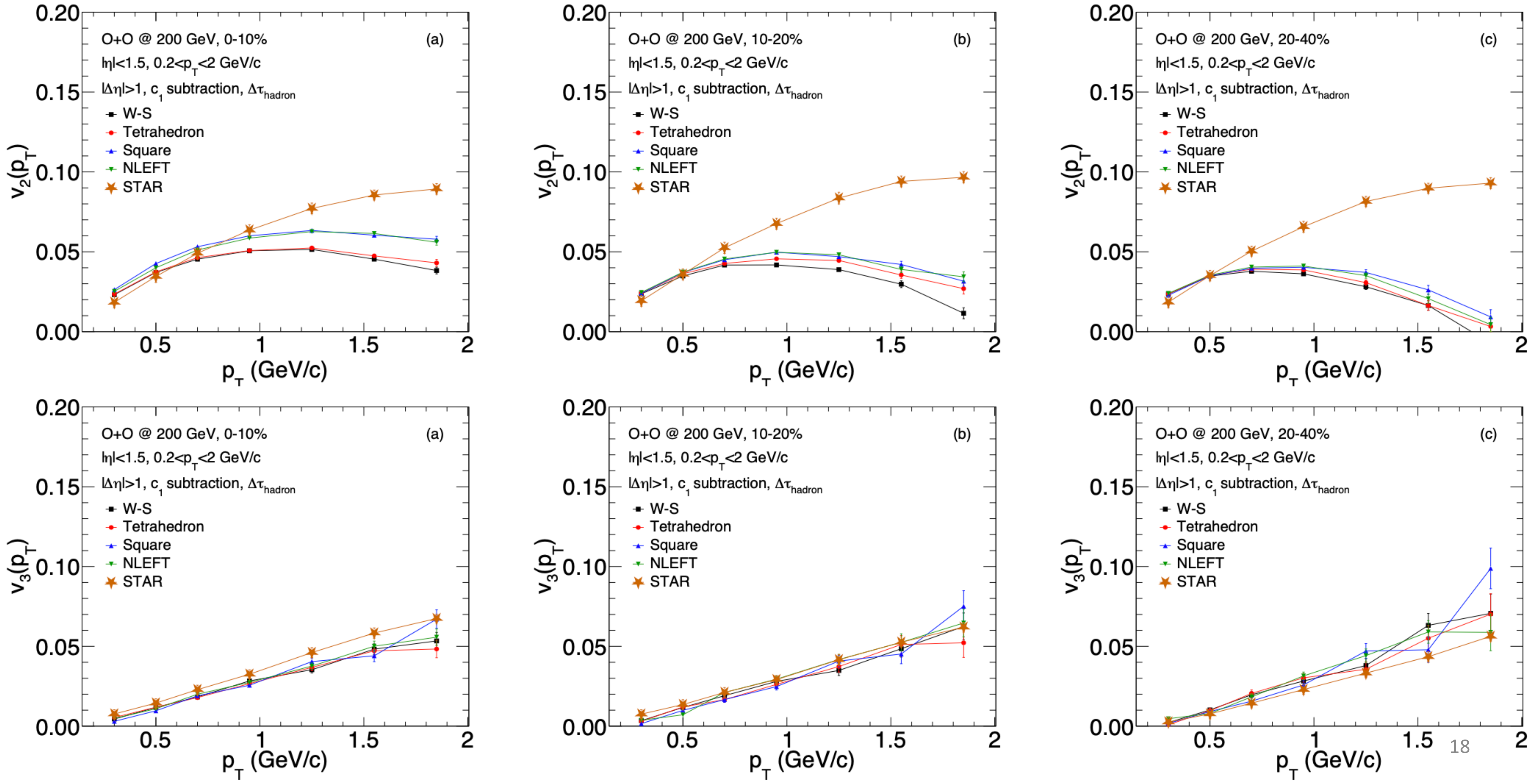

Non-flow effect on $v_n(p_T)$ for $^{16}O+^{16}O$ at 200 GeV

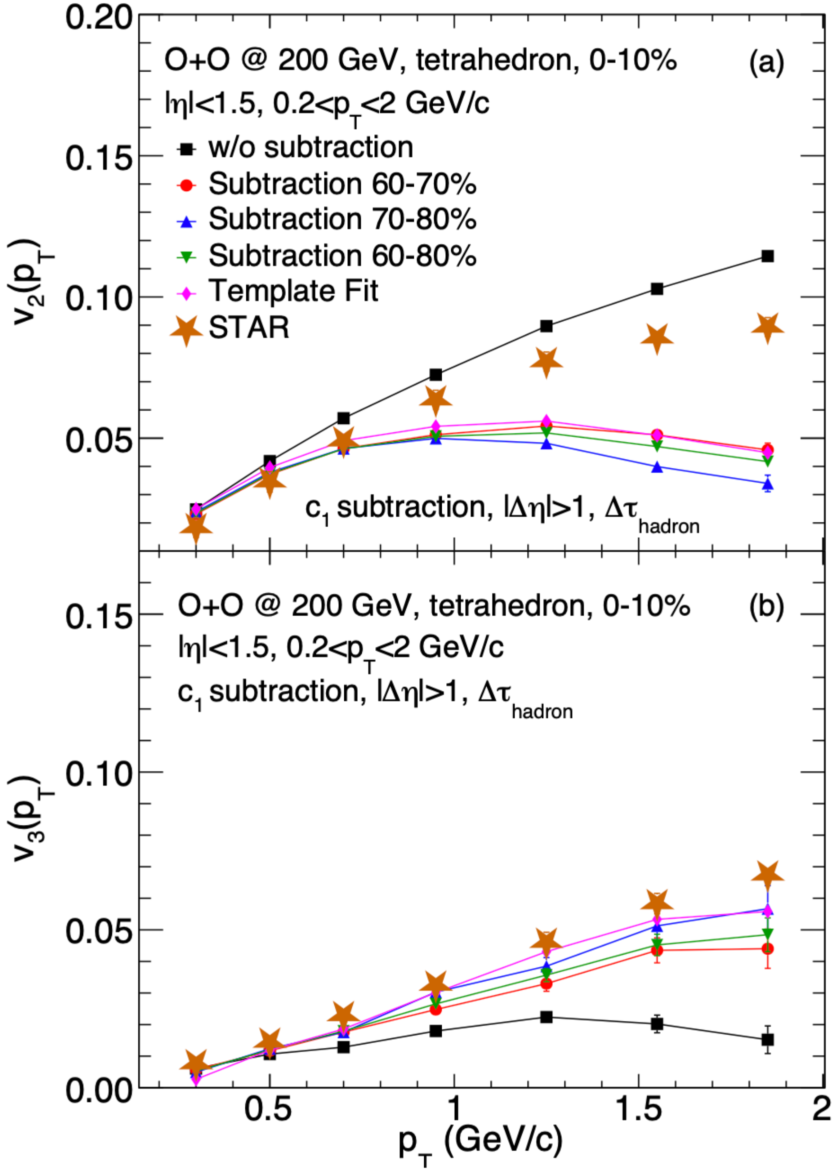

- For $v_2(p_T)$, non-flow may be over-subtracted at high p_{T}.
- The fluctuation induced $v_3(p_T)$ signal is more pronounced after subtracting the more non-flow contribution.

Nuclear Structure for ^{16}O & ^{20}Ne at 5.36 TeV

1) New quark coalescence model
2) Improved heavy quark productions
3) Modern PDFs, nuclear shadowing and Local nuclear scaling

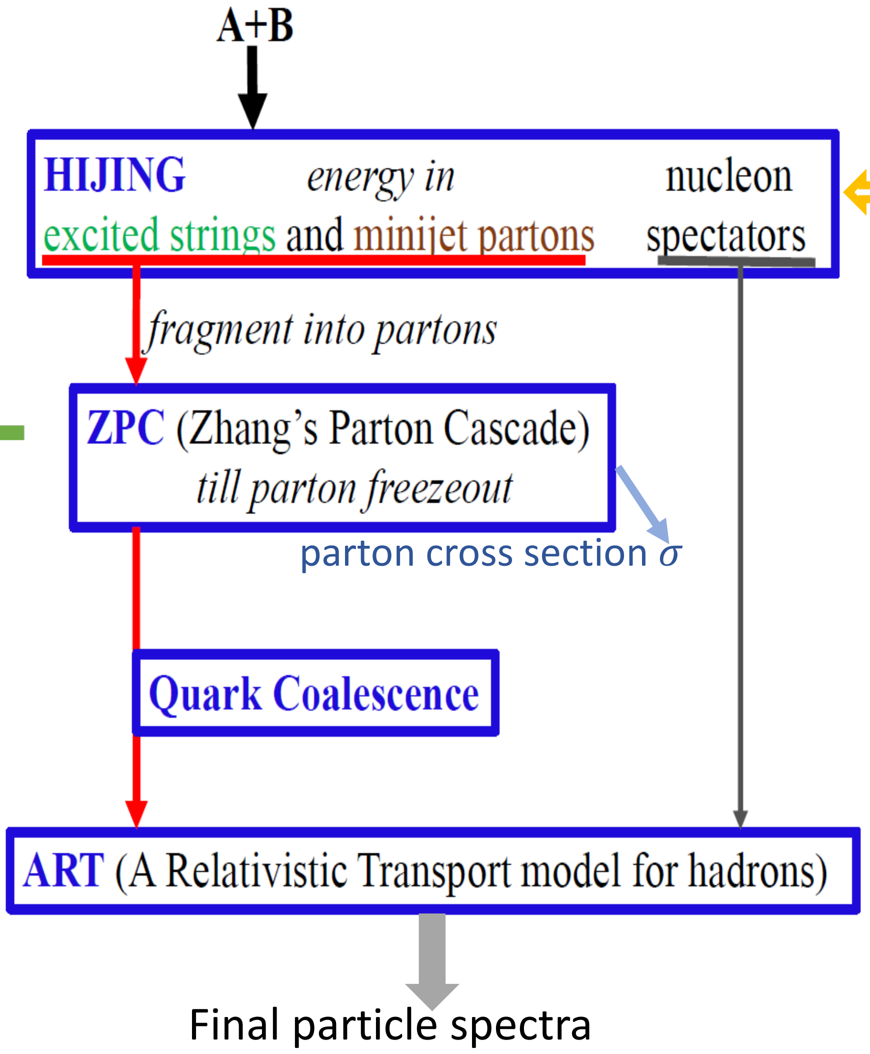

Giuliano Giacalone, et al. arXiv: 2402.05995

1. NLEFT (^{16}O & ^{20}Ne)

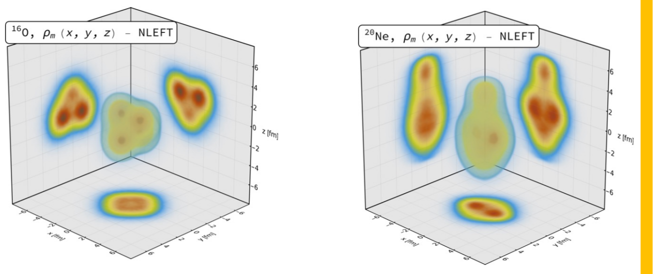

2. PGCM (^{16}O & ^{20}Ne)

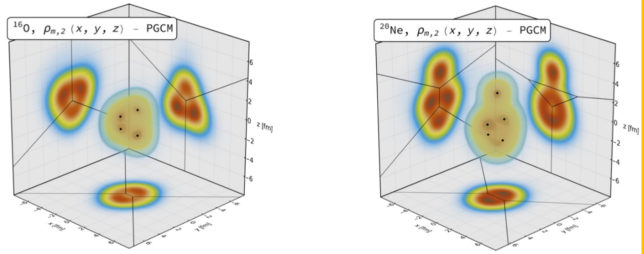

v_n Results for $^{16}O+^{16}O$ & $^{20}Ne+^{20}Ne$ at 5.36 TeV

ALICE, arXiv:2509.06428

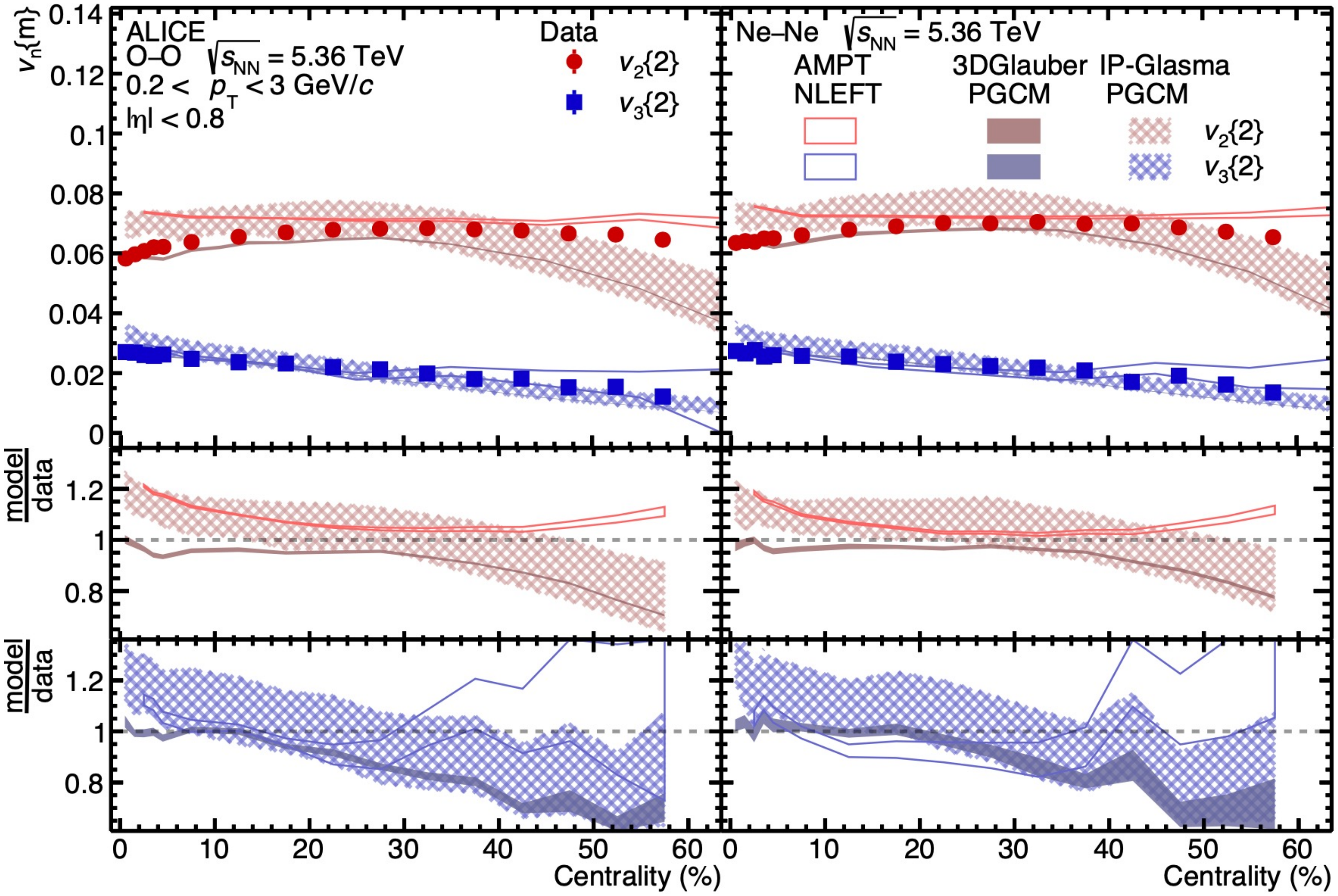

- There are only statistical error bars for the AMPT results.
- Overall, AMPT results are reasonable.
- But the v_2 and v_3 results are too flat.

Prediction Results for $^{16}O+^{16}O$ & $^{20}Ne+^{20}Ne$ at 5.36 TeV

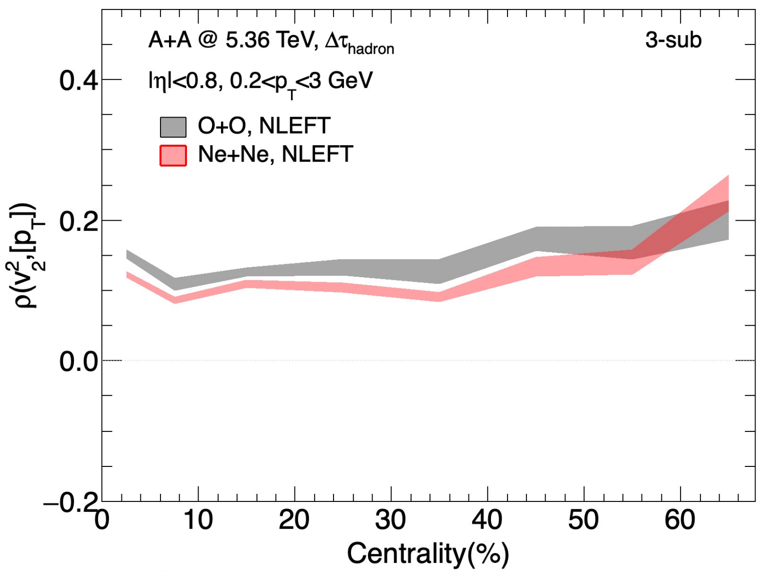

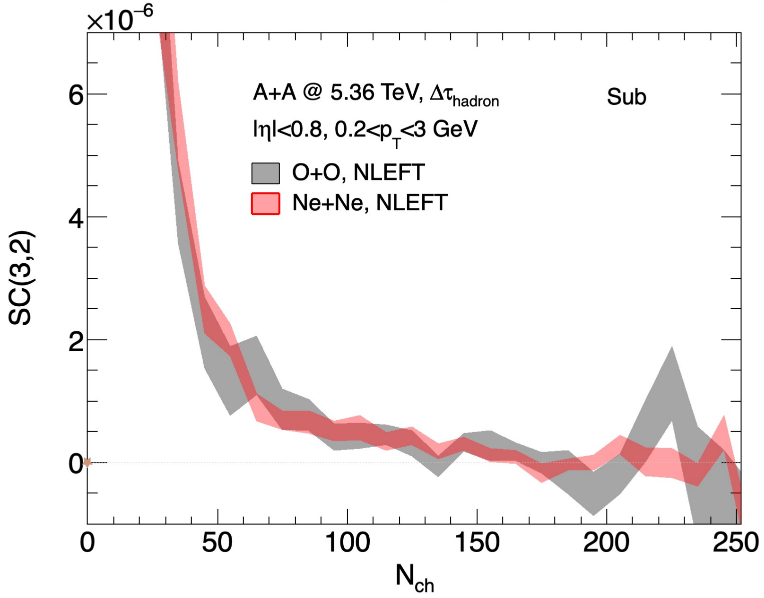

- The positive $\rho(v_2^2, [p_T])$ reflects that events with stronger elliptic flow also have larger radial flow.

- The positive SC(3,2) arises rom the geometry of the cluster structure, which creates a coherent correlation between v_2 and v_3.

Summary & Outlook

- The improved AMPT model can successfully reproduce the STAR and ALICE data for O+O and Ne+Ne collisions.
- Cluster structures have a significant impact on v_2 in the AMPT model.
- Recent developments have made AMPT more accurate and consistent for light-ion collisions.
- To achieve more precise results, future studies will include systematic uncertainties in the AMPT calculations, and further investigations will explore additional light-ion systems and sub-nucleon structure effects.

Summary & Outlook

- The improved AMPT model can successfully reproduce the STAR and ALICE data for O+O and Ne+Ne collisions.
- Cluster structures have a significant impact on v_2 in the AMPT model.
- Recent developments have made AMPT more accurate and consistent for light-ion collisions.
- To achieve more precise results, future studies will include systematic uncertainties in the AMPT calculations, and further investigations will explore additional light-ion systems and sub-nucleon structure effects.

Thank you for your attention!

Backup

Non-flow Methods on $v_n(p_T)$ for ^{16}O+^{16}O at 200 GeV

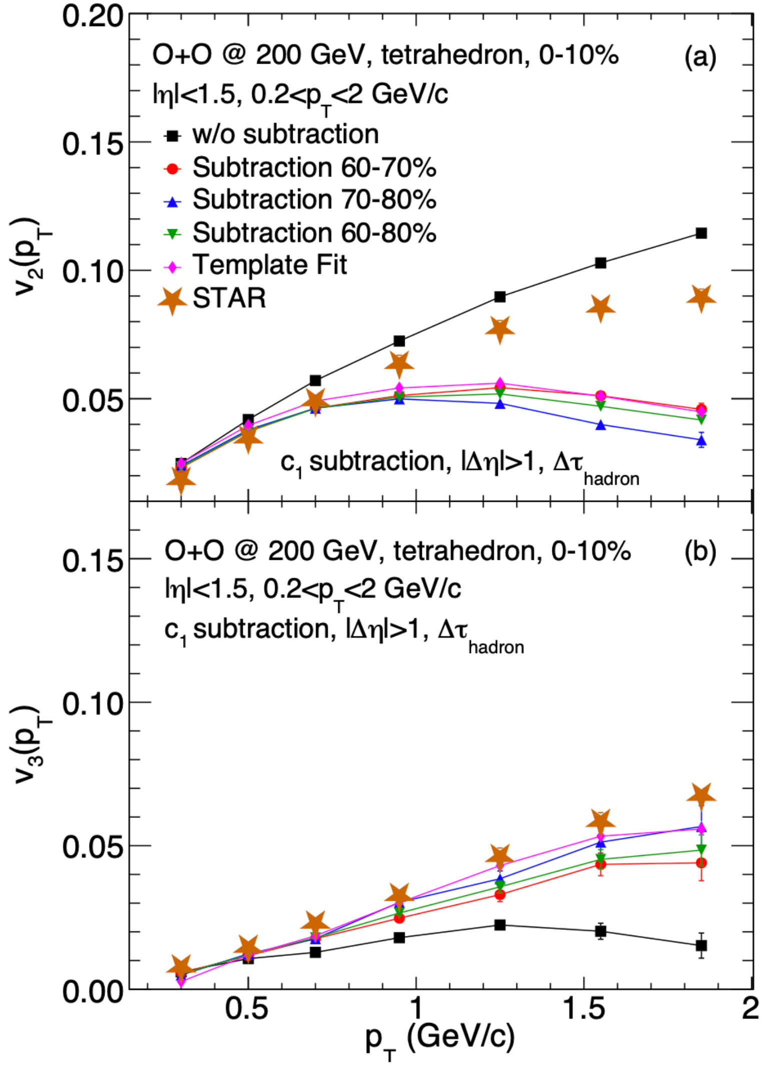

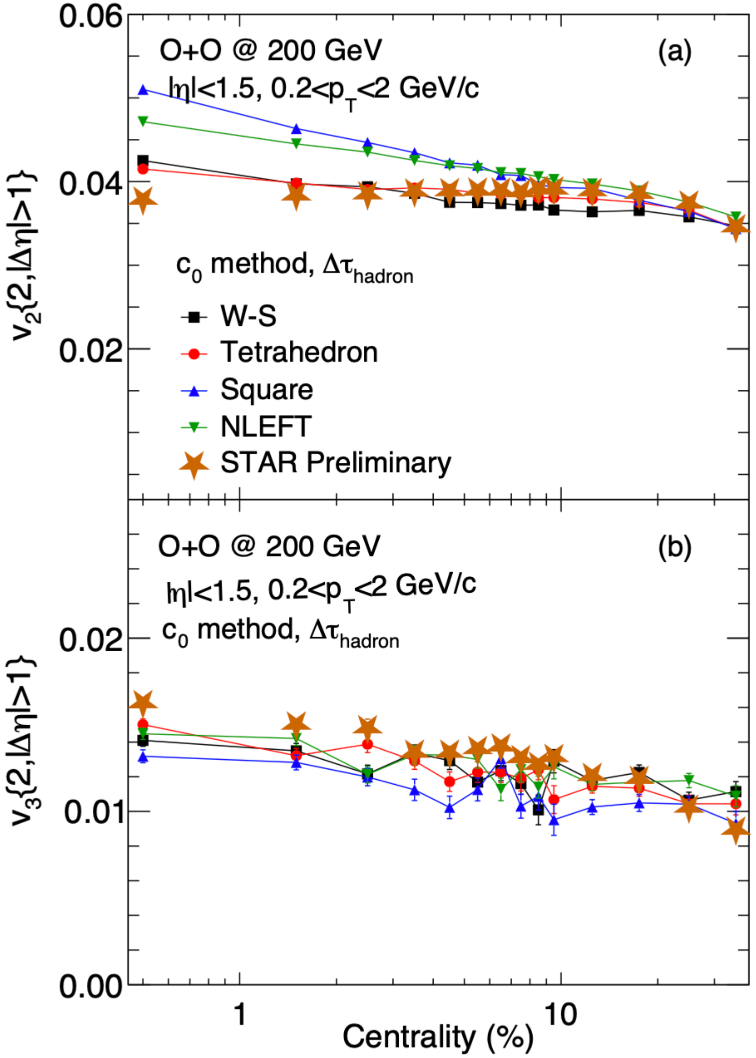

- The non-flow subtraction methods

$$\frac{dN^{\rm pairs}}{d\Delta\phi} \propto 1 + 2\sum_{n=1}^{\infty} v_n \cos(n\Delta\phi)$$

$$Y(\Delta\phi, p_{\rm T}^{\rm trig}) = c_0(1 + 2\sum_{n=1}^{n=4} c_n \cos(n\Delta\phi))$$

$$c_n^{\rm sub} = c_n - c_n^{\rm non-flow} = c_n^{\rm cent} - c_n^{\rm peri} \times f$$

$$f = c_1/c_1^{\rm peri} \ (c_1 \ \text{subtraction})$$

$$f = c_0^{\rm peri}/c_0 \ (c_0 \ \text{subtraction})$$

Results for $^{16}O + ^{16}O$ at 200 GeV

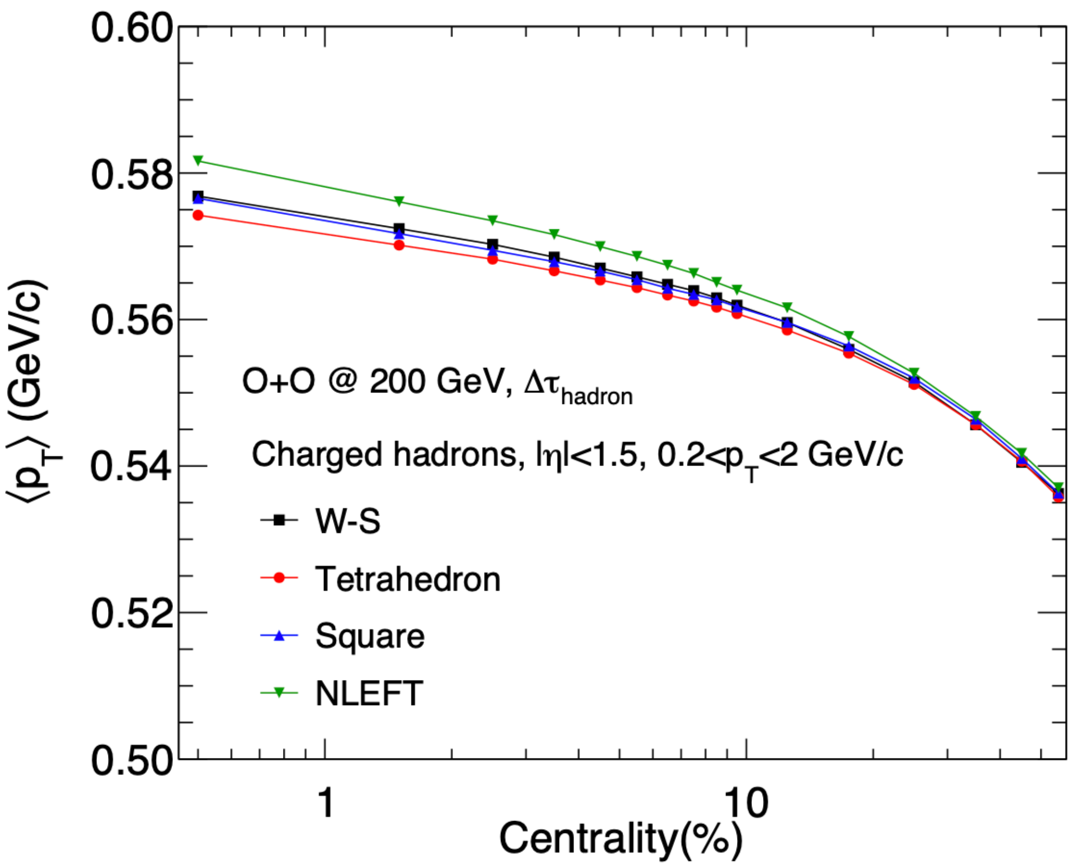

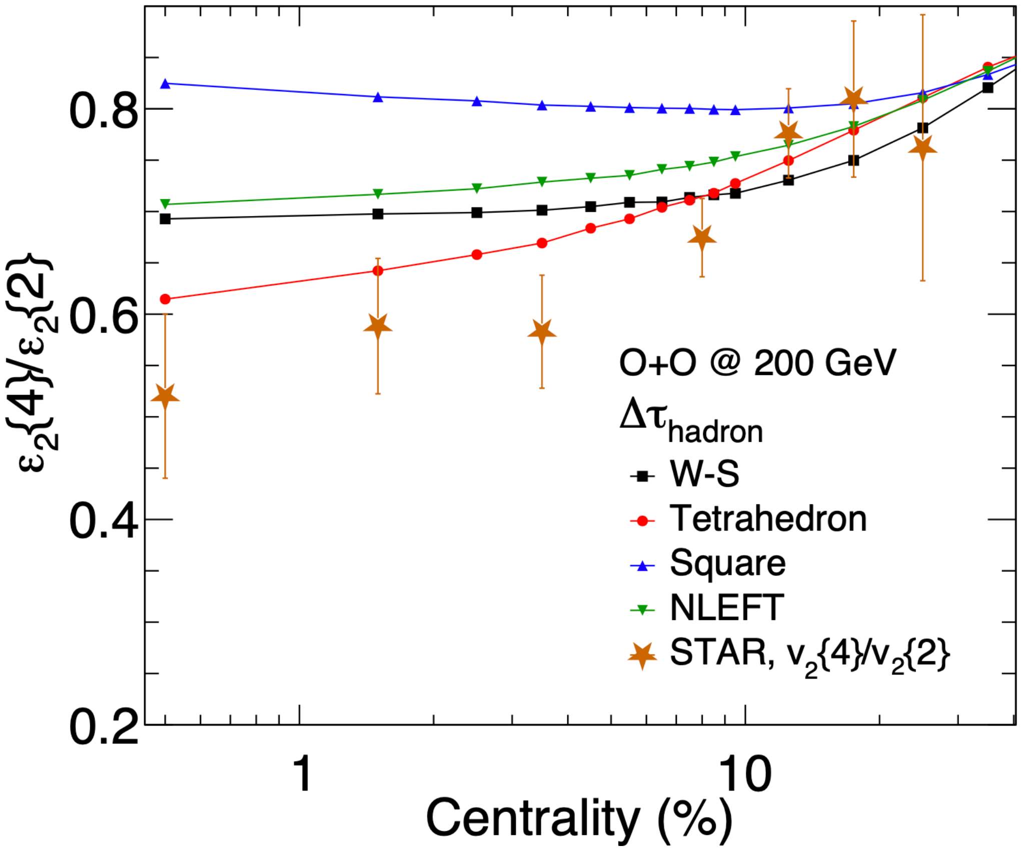

Ratio of v_n at 5.36 TeV

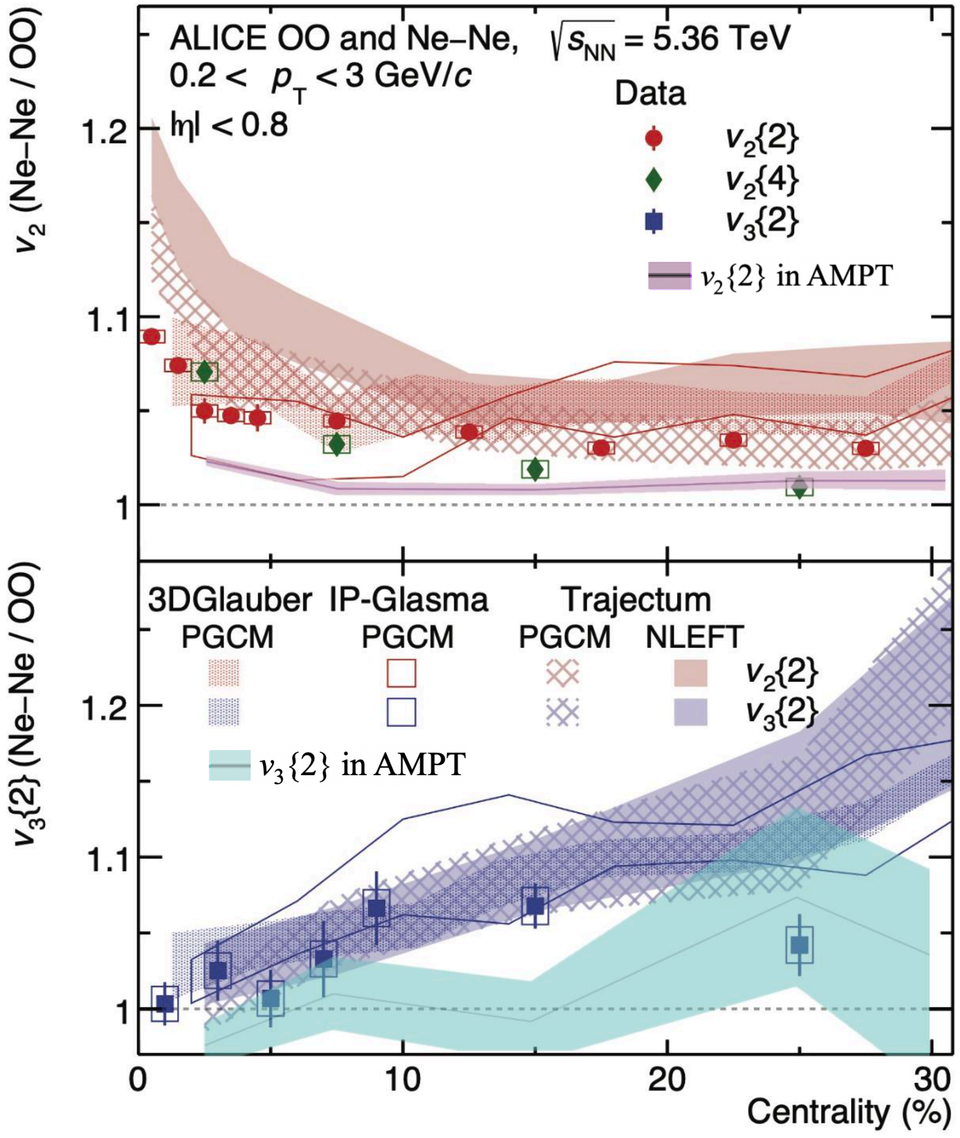

- With statistical errors, the ratio of v_2 & v_3 in AMPT is lower than data.